



Karimi, Nader, Mahmoudi , Yasser, and Mazaheri, Kiumars (2014) Temperature fields in a channel partially filled with a porous material under local thermal non-equilibrium condition: an exact solution. Proceedings of the Institution of Mechanical Engineers Part C: Journal of Mechanical Engineering Science . ISSN 0954-4062

Copyright © 2014 IMechE

A copy can be downloaded for personal non-commercial research or study, without prior permission or charge

Content must not be changed in any way or reproduced in any format or medium without the formal permission of the copyright holder(s)

When referring to this work, full bibliographic details must be given

<http://eprints.gla.ac.uk/91010>

Deposited on: 08 April 2014

Enlighten – Research publications by members of the University of Glasgow_
<http://eprints.gla.ac.uk>

1 **Temperature fields in a channel partially filled with a porous material under local thermal**
2 **non-equilibrium condition-an exact solution**

3

4

Y. Mahmoudi, N. Karimi¹

5

Department of Engineering, University of Cambridge, Cambridge, United Kingdom

6

7 **Abstract**

8 The present work examines analytically the forced convection in a channel partially filled with a porous
9 material and subjected to constant wall heat flux. The Darcy-Brikman-Forchheimer model is used to
10 represent the fluid transport through the porous material. The local thermal non-equilibrium, two-equation
11 model is further employed as the solid and fluid energy equations. Two fundamental models (models A
12 and B) represent the thermal boundary conditions at the interface between the porous medium and the
13 clear region. The governing equations of the problem are manipulated and for each interface model exact
14 solutions, for the solid and fluid temperature fields, are developed. These solutions incorporate the porous
15 material thickness, Biot number, fluid to solid thermal conductivity ratio and Darcy number as
16 parameters. The results can be readily used to validate numerical simulations. They are, further,
17 applicable to the analysis of enhanced heat transfer, using porous materials, in heat exchangers.

18

19 **Key words**

20 porous media, local thermal non-equilibrium, forced convection, heat transfer, exact solution.

21

22 **1. Introduction**

23 The problem of heat transfer enhancement is of rapidly increasing significance [1]. There exist a great
24 number of examples for the heat transfer enhancement by porous materials in natural and manmade

¹ Corresponding author, Department of Engineering, University of Cambridge, CB2 1PZ Cambridge, UK, email:
nk395@cam.ac.uk

1 systems [2]. There is also a significant interest in understanding, modelling and simulation of heat and
2 fluid flow in porous media [2]. This is, in part, to improve the predictive tools used in the design of
3 engineering devices in which porous materials are employed to boost the performance. For instance,
4 porous media are widely used in heat exchangers to enhance the heat transfer rate. Although this usually
5 results in a significant increase in the heat transfer rate, it also causes large pressure drops. To avoid such
6 excessive pressure losses sometimes the fluid conduits are filled only partially with porous materials. Due
7 to the existence of a porous-fluid interface in these partially filled systems, their analysis could be more
8 involved compared to the fully filled ones. Further, the recent technological interests in highly efficient
9 energy systems has intensified the need for more accurate heat transfer analyses [3-5]. Accurate
10 prediction of the flow and temperature fields in the partially filled systems heavily depends upon the
11 proper implementation of the boundary conditions on the porous-fluid interface [6]. These include both
12 hydrodynamic and thermal boundary conditions.

13 In general, two different approaches can be undertaken to apply the conservation of energy in flows
14 through porous media. These include the Local Thermal Equilibrium (LTE) and the Local Thermal Non-
15 Equilibrium (LTNE). LTE model assumes the temperature of the fluid and solid phases are locally the
16 same [6-8]. However, LTNE recognises a finite temperature difference between the two phases. When
17 LTE model is in use, the continuity of temperature and heat flux can be utilised as the boundary
18 conditions at the porous-fluid interface. LTNE model, however, requires implementation of an additional
19 thermal boundary condition at the porous-fluid interface [3, 5-7]. A precise description of the thermal
20 boundary conditions at the porous-fluid interface is yet to be given and the research in this area is ongoing
21 [5, 8]. In the meantime, a number of models have been reported in the literature, which account for the
22 dominant behaviour of the boundary conditions [7]. While these models have been validated against
23 experiments, their applicability is strongly problem dependent and varies with changes in the parameters
24 [7]. The numerical simulations of the partial-porous systems should be, therefore, capable of handling
25 these subtleties. This calls for the comprehensive validation of these tools which, in turn, generates a need
26 for the development of exact solutions of the flow and temperature fields.

1 Analysis of convective heat transfer, in general, includes solution of nonlinear partial differential
2 equations governing the transport of momentum and energy [2]. Hence, it is predominantly feasible
3 through numerical methods. Heat transfer in porous media, however, features certain characteristics that,
4 under some conditions, turn the analysis amenable to the analytical approaches. Utilising these
5 characteristics, this paper reports an analytical analysis of the solid and fluid temperature fields in a
6 system partially filled with a porous insert. This takes into account two different, existing models of the
7 thermal boundary conditions at the porous-fluid interface [7]. Local thermal non-equilibrium model is
8 applied through considering two energy equations for both the fluid phase and the solid matrix. This
9 results in the determination of the temperature fields within the solid and fluid phases. One of the primary
10 aims of the current analysis is to produce a means of validation for the numerical simulations of heat
11 transfer in partially filled systems. The exact solutions, developed in this work, are also of physical
12 significance and can be further employed to evaluate the validity of LTE assumption under varying
13 operating and design parameters.

14 Figure 1 shows the schematic of the problem under investigation. Fluid flows into a channel in which a
15 porous material has been inserted at the core. Constant heat flux boundary condition is applied on the
16 channel walls. Due to the symmetry of this configuration only half of the domain is considered in the
17 analysis. The flow is laminar, steady, thermally and hydrodynamically fully developed, and
18 incompressible. Natural convection, viscous heat generation and radiation heat transfer are ignored.
19 Further, the thermo-physical properties of the fluid and solid are assumed constant.

20

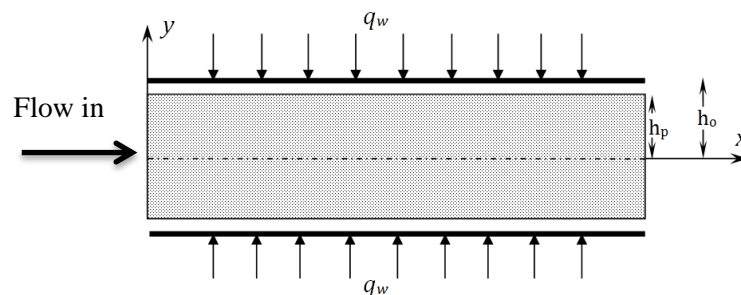


Fig. 1. Schematic of the problem.

1

2. Results and discussions

2.1. Governing equations and the boundary conditions

4 Momentum equation and energy equation in the clear region are respectively expressed by

$$-\frac{\partial p}{\partial x} + \mu \frac{\partial^2 u_f}{\partial y^2} = 0, \quad \rho c_p u_f \frac{\partial T_{f1}}{\partial x} = k_f \frac{\partial^2 T_{f1}}{\partial y^2}. \quad (1a, b)$$

5 Previous investigations [4] have shown that within the porous medium and for $Da < 10^{-3}$, the inertia term
6 of the momentum equation within the porous medium is negligible. Thus, fluid flow through the porous
7 medium is represented by the Darcian flow model. Momentum equation in the porous region reduces to

$$-\frac{\partial p}{\partial x} + \mu_{eff} \frac{\partial^2 u_p}{\partial y^2} - \frac{\mu}{K} u_p = 0. \quad (2)$$

8 Fluid and solid phases energy equations in the porous region are represented by the following coupled
9 partial differential equations

$$0 = k_{s,eff} \frac{\partial^2 T_s}{\partial y^2} - a_{sf} h_{sf} (T_s - T_{f2}), \quad \rho c_p u_p \frac{\partial T_{f2}}{\partial x} = k_{f,eff} \frac{\partial^2 T_{f2}}{\partial y^2} + a_{sf} h_{sf} (T_s - T_{f2}) \quad (3a, b)$$

10 The following boundary conditions are applied to the momentum equations,

$$u_f = 0 \quad \text{at} \quad y = h_0, \quad u_f = u_p, \quad \mu_f \frac{\partial u_f}{\partial y} = \mu_{eff} \frac{\partial u_p}{\partial y} \quad \text{at} \quad y = h_p, \quad \frac{\partial u_p}{\partial y} = 0 \quad \text{at} \quad y = 0. \quad (4a, b, c)$$

11 The boundary conditions applied to the energy equations are

$$\frac{\partial T_{f2}}{\partial y} = \frac{\partial T_s}{\partial y} = 0, \quad \text{at} \quad y = 0, \quad k_f \frac{\partial T_{f1}}{\partial y} = q_w, \quad \text{at} \quad y = h_0, \quad T_{f1} = T_{f2}, \quad \text{at} \quad y = h_p. \quad (5a, b, c)$$

12 In the present work, two models (referred to as A and B in the literature) are utilised to describe the
13 temperature at the interface between the clear and porous regions. Model A was proposed by Vafai and
14 co-workers [8, 9] and is based upon the division of heat flux between the solid and fluid phases and states

$$q_{\text{interface}} = k_{f,eff} \left. \frac{\partial T_f}{\partial y} \right|_{\text{interface}} + k_{s,eff} \left. \frac{\partial T_s}{\partial y} \right|_{\text{interface}}, \quad T_f \Big|_{\text{interface}} = T_s \Big|_{\text{interface}} = T_{\text{interface}}. \quad (6a, b)$$

1 In model B, however, each of the individual phases at the interface receives an equal amount of the heat
 2 flux [8, 9], thus

$$q_{\text{interface}} = k_{f,\text{eff}} \left. \frac{\partial T_f}{\partial y} \right|_{\text{interface}} = k_{s,\text{eff}} \left. \frac{\partial T_s}{\partial y} \right|_{\text{interface}}. \quad (7)$$

3 In the above equations $q_{\text{interface}} = k_f (\partial T_{f1} / \partial y)_{y=h_p}$ and $T_{\text{interface}}$ represents the heat flux and the temperature
 4 at the porous-fluid interface. μ_{eff} is the effective viscosity of the porous medium which is considered equal
 5 to μ_f [10]. The average velocity in the channel is $\bar{u} = 1/h_0 \{ \int_0^{h_p} u_p dy + \int_{h_p}^{h_0} u_f dy \}$. Integrating Eq. (1b) from h_p
 6 to h_0 and noting that in the fully developed region $\partial T_{f1} / \partial x = \partial T_{f2} / \partial x = \partial T_f / \partial x$ are constants, result in

$$\rho c_p \frac{\partial T_f}{\partial x} \int_{h_p}^{h_0} u_f dy = (q_w - q_{\text{interface}}). \quad (8)$$

7 Adding Eqs. (3a) to (3b), integrating the sum from 0 to h_p and applying the boundary conditions given by
 8 Eqs. (6a) and (6b) reveal the following equation for model A

$$\rho c_p \frac{\partial T_f}{\partial x} \int_0^{h_p} u_p dy = q_{\text{interface}}. \quad (9)$$

9 Adding Eq. (8) to Eq. (9) and using the definition of the average velocity yield

$$\rho c_p \left. \frac{\partial T_f}{\partial x} \right|_{\text{ModelA}} = \frac{q_w}{h_0} \frac{1}{\bar{u}}. \quad (10)$$

10 Substituting Eq. (10) into Eq. (9) renders model A prediction of heat flux at the porous medium-fluid
 11 interface as,

$$\left. \frac{q_{\text{interface}}}{q_w} \right|_{\text{ModelA}} = \frac{1}{h_0 \bar{u}} \int_0^{h_p} u_p dy. \quad (11)$$

12 Through adding Eqs. (3a) to (3b), integrating the sum from 0 to h_p and applying boundary condition (7)
 13 (model B) the following equation is obtained,

$$\rho c_p \frac{\partial T_f}{\partial x} \int_0^{h_p} u_p dy = 2q_{\text{interface}}. \quad (12)$$

14 Adding Eq. (8) to Eq. (12) and using the definition of average velocity result in

$$\rho c_p \left. \frac{\partial T_f}{\partial x} \right|_{\text{ModelB}} = \frac{1}{h_0 \bar{u}} (q_w + q_{\text{interface}}). \quad (13)$$

1 An explanation can be given for Eq. (12). The heat flux $q_{\text{interface}}$ from the outer surface is transferred to the
 2 porous medium in two different ways. First, conduction in the fluid phase, q_f , and second, conduction in
 3 the solid phase, q_s . Model B states that each phase receives the same amount of heat flux, which is equal
 4 to $q_{\text{interface}}$. Thus $q_f = q_{\text{interface}}$ and $q_s = q_{\text{interface}}$. This is in keeping with the second approach of Amiri et. al
 5 [9]. The heat transferred to the solid phase is ultimately delivered to the fluid through an internal heat
 6 exchange. This heat exchange is, therefore, equal to the heat transferred from the wall to the solid phase
 7 via solid conduction, $q_{\text{exchange}} = q_s$ [11]. It follows that the overall heat transfer to the fluid phase in the
 8 porous region is by direct fluid conduction plus the solid conduction and the subsequent internal heat
 9 exchange between the solid and fluid. Thus, $q_{\text{total,fluid,porous}} = q_{\text{interface}} + q_{\text{interface}} = 2 q_{\text{interface}}$.

10 Substituting Eq. (13) into Eq. (12) reveals model B prediction of the heat flux at the porous medium-
 11 fluid interface,

$$\left. \frac{q_{\text{interface}}}{q_w} \right|_{\text{ModelB}} = \frac{\int_0^{h_p} u_p dy}{2h_0 \bar{u} - \int_0^{h_p} u_p dy}. \quad (14)$$

12 To normalise the governing equations and boundary conditions the following dimensionless variables are
 13 introduced.

$$\Theta|_{\text{ModelA}} = \frac{k_{s,eff} (T - T_{\text{interface}})}{q_w h_0}, \Theta|_{\text{ModelB}} = \frac{k_{s,eff} (T - T_{s,\text{interface}})}{q_w h_0}, \gamma = \frac{q_{\text{interface}}}{q_w}, k = \frac{k_{s,eff}}{k_{f,eff}}, \quad (15a, b, c, d)$$

$$Bi = \frac{a_{sf} h_{sf} h_0^2}{k_{s,eff}}, Y = \frac{y}{h_0}, S = \frac{h_p}{h_0}, U = \frac{u}{u_r}, \quad (15e, f, g, h)$$

14 where u_r is a characteristic velocity defined as $u_r = -(h_0^2 / \mu)(\partial p / \partial x)$. The solutions for the momentum
 15 Eqs. (1a) and (1b) and the corresponding boundary conditions (4a), (4b), and (4c) are as follows. For the
 16 clear region

$$U_f(Y) = -\frac{1}{2} Y^2 + AY + B, \quad (16a)$$

$$A = S + \frac{Z \sinh(ZS)(S - 0.5 \times (1 + S^2) + Da)}{Z(S - 1) \sinh(ZS) - \cosh(ZS)}, \quad B = 1/2 - S - \frac{Z \sinh(ZS)(S - 0.5 \times (1 + S^2) + Da)}{Z(S - 1) \sinh(ZS) - \cosh(ZS)}. \quad (16b, c)$$

1 Within the porous region

$$U_p = C \cosh(ZY) + Da, \quad C = \frac{1}{Z \sinh(ZS)} \times (A - S). \quad (17a, b)$$

2 By using Eqs. (16a, b, c) and (17a, b) and dimensionless parameters in relation (15a-h) the dimensionless
3 average velocity becomes

$$\bar{U} = SDa + \frac{D}{Z} \sinh(ZS) - \frac{1}{6}(1 - S^3) + \frac{1}{2}A(1 - S^2) + B(1 - S), \quad (18)$$

4 where $Z = \sqrt{1/Da}$, S is the ratio of the porous medium thickness to the channel height.

5 Equation (11) is converted to non-dimensional form and is combined with Eqs. (17a, b) and (18)
6 revealing

$$\gamma|_{\text{ModelA}} = \frac{1}{\bar{U}} \int_0^s U_p dY, \quad \gamma|_{\text{ModelA}} = \frac{\frac{D}{Z} \sinh(ZS) + SDa}{SDa + \frac{D}{Z} \sinh(ZS) - \frac{1}{6}(1 - S^3) + \frac{1}{2}A(1 - S^2) + B(1 - S)}. \quad (19a, b)$$

7 Similar to that explained in the derivation of Eq. (19b), an expression for the heat flux at the porous
8 medium-fluid interface for model B, is obtained as

$$\gamma|_{\text{ModelB}} = \frac{\int_0^s U_p dY}{2\bar{U} - \int_0^s U_p dY}. \quad (20)$$

9 Once again, by using Eqs. (16a, b, c) and (17a, b) it can be shown that

$$\gamma|_{\text{ModelB}} = \frac{\frac{D}{Z} \sinh(ZS) + SDa}{2(SDa + \frac{D}{Z} \sinh(ZS) - \frac{1}{6}(1 - S^3) + \frac{1}{2}A(1 - S^2) + B(1 - S)) - \frac{D}{Z} \sinh(ZS) + SDa}. \quad (21)$$

10

11 2.2. Temperature profile for model A

12 The energy equations and the associated boundary conditions are derived through substitution of the
13 dimensionless variables presented in Eqs. (15a-d) into Eqs. (2), (3a) and (3b). Dimensionless energy
14 equation for the fluid in the clear and porous regions become

$$\varepsilon k \frac{U_f}{U} = \Theta''_{f1}(Y), \quad \frac{U_p}{U} = \frac{1}{k} \Theta''_{f2}(Y) + Bi(\Theta_s(Y) - \Theta_{f2}(Y)). \quad (22a, b)$$

1 The solid phase energy equation in the porous region can be written as

$$0 = \Theta''_s(Y) - Bi(\Theta_s(Y) - \Theta_{f2}(Y)). \quad (23)$$

2 The boundary conditions of the energy equations are

$$\Theta'_{f1}(1) = \varepsilon k, \quad \Theta_{f1}(S) = \Theta_{f2}(S) = \Theta_s(S) = 0, \quad \Theta'_{f2}(0) = \Theta'_s(0) = 0. \quad (24a, b, c)$$

3 Applying Eqs. (22b) and (23) at $Y=S$ yields

$$\frac{U_p(S)}{U} = \frac{1}{k} \Theta''_{f2}(S) + Bi(\Theta_s(S) - \Theta_{f2}(S)), \quad 0 = \Theta''_s(S) - Bi(\Theta_s(S) - \Theta_{f2}(S)). \quad (25a, b)$$

4 Using boundary condition (24b) (i.e. $\Theta_{f2}(S) = \Theta_s(S) = 0$), Eqs. (25a) and (25b) are converted to

$$\Theta''_{f2}(S) = k \frac{U_p(S)}{U}, \quad \Theta''_s(S) = 0. \quad (26a, b)$$

5 Differentiation of Eqs. (22b) and (23) with respect to Y and evaluating the results at $Y=0$ yield

6

$$\Theta'''_{f2}(0) = k \frac{U'_p(0)}{U} = \frac{0}{U} = 0, \quad \Theta'''_s(0) = 0. \quad (27a, b)$$

7 Differentiating Eqs. (22b) and (23) with respect to Y for two times gives

$$\frac{U''_p(Y)}{U} = \frac{1}{k} \Theta'''_{f2}(Y) + Bi(\Theta''_s(Y) - \Theta''_{f2}(Y)), \quad 0 = \Theta'''_s(Y) - Bi(\Theta''_s(Y) - \Theta''_{f2}(Y)). \quad (28a, b)$$

8 Adding Eq. (22b) to Eq. (23) results in the following second order differential equation

$$\frac{U_p}{U} = \frac{1}{k} \Theta''_{f2}(Y) + \Theta''_s(Y). \quad (29)$$

9 By writing $\Theta''_s(Y)$ as $\Theta''_{f2}(Y)$ and substituting the result into Eq. (28a) we arrive at

$$\Theta'''_{f2}(Y) - Bi(1+k)\Theta''_{f2}(Y) = \frac{k}{U} (-BiU_p(Y) + U''_p(Y)), \quad (30)$$

10 and similarly writing $\Theta''_{f2}(Y)$ as $\Theta''_s(Y)$ and substituting the result into Eq. (28b) lead to

$$\Theta'''_s(Y) - Bi(1+k)\Theta''_s(Y) = -\frac{k}{U} BiU_p(Y). \quad (31)$$

1 Equations (30) and (31) are two decoupled ordinary differential energy equations representing the
 2 transport of energy in the porous region. Integrating the ordinary differential Eq. (22a) results in the
 3 following expression for the temperature distribution of the flow in the clear region under model A

$$\Theta_{f1}(Y)|_{\text{ModelA}} = \frac{\varepsilon k}{U} \left(-\frac{Y^4}{24} + A\frac{Y^3}{6} + B\frac{Y^2}{2} + \left(\frac{1}{6} - \frac{A}{2} - B + \bar{U} \right) Y + \frac{S^4}{24} - A\frac{S^3}{6} - B\frac{S^2}{2} - S \left[\frac{1}{6} - \frac{A}{2} - B + \bar{U} \right] \right), \quad (32)$$

4 where A and B are given by Eqs. (16b) and (16c). The temperature distribution in the porous region is
 5 found by solving Eqs. (30) and (31) and applying the boundary conditions given by Eqs. (24) and (27).
 6 This reveals

$$\Theta_{f2}(Y)|_{\text{ModelA}} = \frac{k}{U} \left\{ \frac{C(Z^2 - Bi) \times [\cosh(ZY) - \cosh(ZS) \times (1 + \xi \times Z^2)]}{Z^2(-\Gamma^2 + Z^2)} + \frac{Da Bi}{\Gamma^2} \times \left(-\xi + \frac{Y^2}{2} - \frac{S^2}{2} \right) + U_p(S)\xi \right\}, \quad (33)$$

$$\Theta_s(Y)|_{\text{ModelA}} = -Bi \frac{k}{U} \left\{ \frac{C[\cosh(ZY) - \cosh(ZS) \times (1 + \xi \times Z^2)]}{Z^2(-\Gamma^2 + Z^2)} - \frac{Da}{\Gamma^2} \left(-\xi + \frac{Y^2}{2} - \frac{S^2}{2} \right) \right\}, \quad (34)$$

7 where $\Gamma = \sqrt{Bi(1+k)}$ and $\xi = \left(\frac{\cosh(\Gamma Y)}{\cosh(\Gamma S)} - 1 \right) / \Gamma^2$.

8

9 **2.3. Temperature profile for model B**

10 Substitution of Eq. (15a) into Eqs. (2), (3a) and (3b) reveals the different forms of the energy equation for
 11 the two phases based on model B. Energy equation for the fluid in the clear region then becomes

$$\varepsilon k \left(1 + \frac{1}{\gamma} \right) \frac{U_f}{U} = \Theta_{f1}''(Y). \quad (35)$$

12 Further, fluid and solid phase energy equations in the porous region take respectively the forms of

$$\frac{U_p}{U} = \frac{1}{k} \Theta_{f2}''(Y) + Bi(\Theta_s(Y) - \Theta_{f2}(Y)), \quad 0 = \Theta_s''(Y) - Bi(\Theta_s(Y) - \Theta_{f2}(Y)). \quad (36a, b)$$

13 The associated boundary conditions are

$$\Theta'_{f_1}(1) = \varepsilon k, \quad \Theta_{f_1}(S) = \Theta_{f_2}(S), \quad \Theta'_{f_2}(0) = \Theta'_s(0) = 0, \quad (37a, b, c)$$

$$\Theta'_{f_2}(s) = \frac{k}{\gamma}, \quad \Theta'_s(s) = \frac{1}{\gamma}, \quad \Theta''_s(s) + Bi \Theta_{f_2}(s) = 0, \quad \Theta_s(s) = 0. \quad (37d, e, f, g)$$

- 1 Following the same procedure explained for model A, and taking the second derivative of Eqs. (36a) and
- 2 (36b) with respect to Y , yield

$$\Theta''''_{f_2}(Y) - Bi(1+k)\Theta''_{f_2}(Y) = \frac{k}{U} \left(1 + \frac{1}{\gamma}\right) (-BiU_p(Y) + U''_p(Y)), \quad (38a)$$

$$\Theta''_s(Y) - Bi(1+k)\Theta''_s(Y) = -\frac{k}{U} \left(1 + \frac{1}{\gamma}\right) BiU_p(Y). \quad (38b)$$

- 3 Evaluating the second and third derivatives of Θ_s and Θ_{f_2} at the symmetry plane ($Y=0$) by applying Eq.
- 4 (37c) reveals

$$\Theta'''_{f_2}(0) = k \frac{U'_p(0)}{U} = 0, \quad \Theta'''_s(0) = 0. \quad (39a, b)$$

- 5 Solving the ordinary differential Eq. (35) results in the following expressions for the temperature
- 6 distribution for the flow in the clear region

$$\Theta_{f_1}(Y) \Big|_{\text{ModelB}} = \varepsilon \psi \left(-\frac{1}{24} Y^4 + A \frac{Y^3}{6} + B \frac{Y^2}{2} + O_1 Y + O_2 \right), \quad (40a)$$

$$O_1 = \frac{k}{\psi} - \left(-\frac{1}{6} + \frac{A}{2} + B \right), \quad O_2 = \frac{\Theta_{f_2}(s)}{\varepsilon \psi} - \left(-\frac{1}{24} S^4 + A \frac{S^3}{6} + B \frac{S^2}{2} + O_1 S \right), \quad (40b, c)$$

- 7 where $\psi = (k/\bar{U})(1+1/\gamma)$ and, A and B are respectively given by Eqs. (16b) and (16c). The temperature
- 8 distribution in the porous region is found by solving Eqs. (38a) and (38b) and applying Eqs. (37) and (39).
- 9 These render

$$\Theta_{f_2}(Y) \Big|_{\text{ModelB}} = \frac{\phi 1}{\Gamma^2} \cosh(\Gamma Y) + \frac{Bi Da \psi}{\Gamma^2} \frac{Y^2}{2} - \frac{C \psi (Z^2 - Bi)}{Z^2 (Z^2 - \Gamma^2)} \cosh(ZY) + \phi 2, \quad (41)$$

$$\Theta_s(Y)|_{\text{Model B}} = \frac{\phi_3}{\Gamma^2} [\cosh(\Gamma Y) - \cosh(\Gamma S)] + \frac{Bi Da \psi}{\Gamma^2} \left[\frac{Y^2}{2} - \frac{S^2}{2} \right] - \frac{Bi C \psi}{Z^2 (Z^2 - \Gamma^2)} [\cosh(ZY) - \cosh(ZS)], \quad (42)$$

1 where

$$\phi_1 = \frac{\Gamma}{\sinh(\Gamma S)} \left[\frac{k}{\gamma} - \frac{Bi Da \psi}{\Gamma^2} S - \frac{C \psi (Z^2 - Bi)}{Z (Z^2 - \Gamma^2)} \sinh(ZS) \right], \quad (43a)$$

$$\phi_2 = \frac{\Gamma}{\sinh(\Gamma S)} \left[\frac{1}{\gamma} - \frac{Bi Da \psi}{\Gamma^2} S + \frac{Bi C \psi}{Z (Z^2 - \Gamma^2)} \sinh(ZS) \right], \quad (43b)$$

$$\phi_3 = \cosh(\Gamma S) \left[-\frac{\phi_1}{\Gamma^2} - \frac{\phi_2}{Bi} \right] + \frac{Bi Da \psi}{\Gamma^2} \left(-\frac{1}{Bi} - \frac{S^2}{2} \right) + \frac{Bi C \psi}{Z^2 (Z^2 - \Gamma^2)} \cosh(ZS), \quad (43c)$$

$$\psi = \frac{k}{U} \left(1 + \frac{1}{\gamma} \right), \quad \Gamma = \sqrt{Bi(1+k)}. \quad (43d)$$

2 2.4. Validation

3 To validate the present exact solutions, temperature distributions in the solid and fluid phases are
4 evaluated for a channel fully filled with a porous material. In Eqs. (33) and (34) for model A and Eqs.
5 (41) and (42) for model B, S is set equal to one. The obtained results are compared against the exact
6 solutions derived by Marafie and Vafai [12] and Yang and Vafai [7]. The excellent agreement between
7 these solutions, shown in Fig. 2, confirms the validity of the presented analysis.

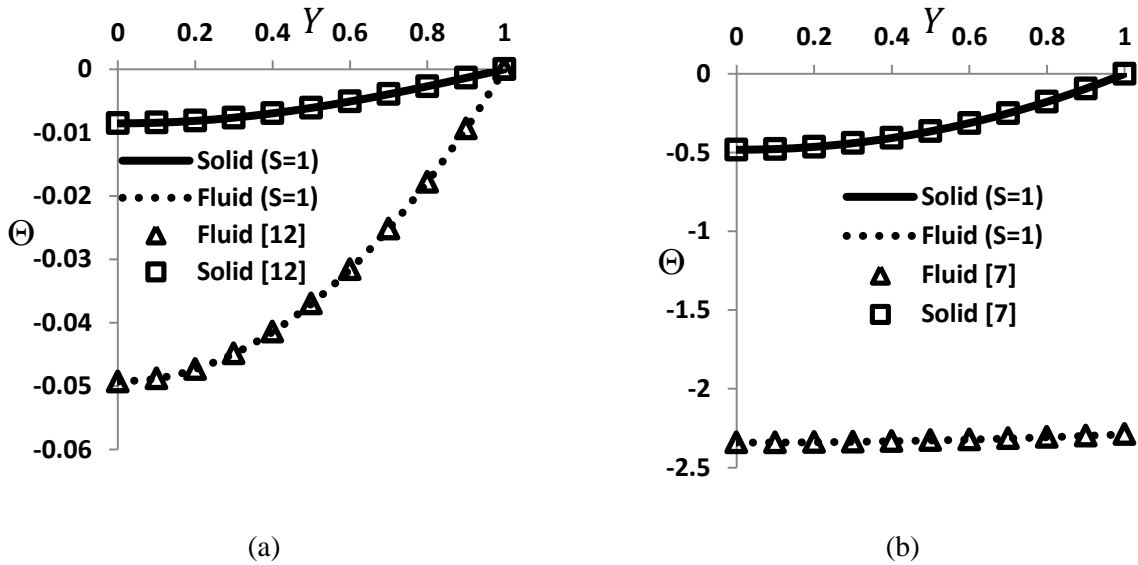


Fig. 2. Temperature distributions in the fluid and solid phases for $S=1$, $k=0.01$, $Bi=10$ and $Da=10^{-4}$. Solid lines: present solutions, symbols: exact solutions in [7, 12], (a) model A, Eqs. (33) and (34) and, (b) model B, Eqs. (41) and (42).

1

2 3. Conclusions

3 Temperature fields of the solid and fluid phases in a channel partially filled with a porous medium under
 4 local thermal non-equilibrium condition were investigated analytically. The coupled partial differential
 5 equations for the transport of momentum and energy in a fluid flow through a porous medium, along with
 6 the energy balance of the solid matrix were considered. These were first converted to a set of decoupled
 7 ordinary differential equations and were subsequently solved analytically. Further, two distinctive thermal
 8 boundary conditions (the so-called models A and B) were applied to the interface between the porous
 9 medium. Model A assumes that heat is divided between the two phases on the basis of their effective
 10 conductivities and their corresponding temperature gradients. Model B, however, assumes that both
 11 phases at the interface receive the same amount of heat flux. Exact solutions were developed for the solid
 12 and fluid phases. These solutions are of direct use in the analysis of heat transfer enhancement as well as
 13 the validation of numerical simulations under varying parameters. In addition, the present set of results
 14 can be used as a supplement in the numerical simulations of the more involved problems. This is to
 15 reduce the computational burden of solving the momentum and energy equations. An example of such
 16 problems is the analysis of reactive flows in porous media.

17

18 Nomenclature

a_{sf}	Interfacial area per unit volume of porous media (m^{-1})	x	Longitudinal coordinate (m)
A, B	Constant parameter defined by Eq. (16b, c)	y	Transverse coordinate (m)
Bi	Biot number,	Y	Dimensionless y coordinate, y/h_0

C	Constant parameter defined by Eq. (17b)	Z	Constant parameter, $\sqrt{1/Da}$
C_p	Specific heat of the fluid, (J Kg ⁻¹ k ⁻¹)	<i>Greek symbols</i>	
Da	Darcy number, K/h_0^2	γ	Ratio of wall heat flux to the heat flux at the interface, $q_w/q_{interface}$
h_{sf}	Fluid to solid heat transfer coefficient (W m ⁻² k ⁻¹)	Γ	Constant parameter defined by Eq. (43d)
h_0	Height of the channel (m)	ε	Porosity of the porous medium
h_p	Porous substrate thickness (m)	Θ	Dimensionless temperature
K	Permeability of the porous medium (m ²)	μ	Viscosity (Kg m ⁻¹ s ⁻¹)
k	The ratio of solid effective thermal conductivity to that of the fluid, $(1-\varepsilon)k_s/(\varepsilon k_f)$	ρ	Density, (kg/m ³)
k_f	Thermal conductivity of the fluid (W m ⁻¹ k ⁻¹)	ξ	Constant parameter used in Eq. (34)
$k_{f,eff}$	Effective thermal conductivity of the fluid, εk_f	ψ	Constant parameter defined by Eq. (43d)
k_s	Thermal conductivity of the solid (W m ⁻¹ k ⁻¹)	$\phi 1, \phi 2, \phi 3$	Constant parameter defined by Eq. (43a, b, c)
$k_{s,eff}$	Effective thermal conductivity of the solid, $(1-\varepsilon)k_s$	<i>Subscripts</i>	
O_1, O_2	Constant parameter defined by Eq. (40b, c)	eff	Effective property
p	Pressure (Pa)	f	Fluid
q	Heat flux (W m ⁻²)	$f1$	Fluid in the clear region
S	Ratio of the porous medium thickness to the	$f2$	Fluid in the porous medium

	channel height, h_p/h_0		
T	Temperature (K)	<i>Superscripts</i>	
u	Longitudinal velocity (m/s)	–	Mean value
U	Dimensionless velocity, u/u_r	′, ″, ‴, ″″	First, second, third, and fourth derivatives

1

2 References

- [1] Webb, R.L., Kim, N. *Principles Of Enhanced Heat Transfer*, 2nd edition, New York, Taylor & Francis, 2005.
- [2] Vafai, K., *Handbook of porous media*, 2nd edition, New York, Marcel Dekker, 2000.
- [3] Mahmoudi, Y., Maerefat M. Analytical investigation of heat transfer enhancement in a channel partially filled with a porous material under local thermal non-equilibrium condition. *Int. J. Thermal Sciences* 2011; 50: 2386-2401.
- [4] Maerefat, M., Mahmoudi, S.Y., Mazaheri, K., Numerical simulation of forced convection enhancement in a pipe by porous inserts. *Int. J. Heat Transfer Engineering* 2011; 32: 45-56.
- [5] Yang, K., Vafai, K. Restrictions on the validity of the thermal conditions at the porous-fluid interface: an exact solution. *ASME J. Heat Transfer* 2011c; 133: 112601-12.
- [6] Yang, K., Vafai, K. Analysis of heat flux bifurcation inside porous media incorporating inertial and dispersion effects – an exact solution. *Int. J. Heat Mass Transfer* 2011b; 54: 5286–5297.
- [7] Yang, K., Vafai, K. Analysis of temperature gradient bifurcation in porous media – an exact solution. *Int. J. Heat Mass Transfer* 2010; 53: 4316–4325.
- [8] Alazmi, B., Vafai, K. Constant wall heat flux boundary conditions in porous media under local thermal non-equilibrium conditions. *Int. J. Heat Mass Transfer* 2002; 45: 3071-3087.
- [9] Amiri, A., Vafai, K., Kuzay, T.M. Effect of Boundary Conditions on Non-Darcian Heat Transfer Through Porous Media and Experimental Comparisons. *Numerical Heat Transfer Journal* 1995,

Part A; 27: 651-664.

- [10] Alazmi, B., Vafai K. Analysis of fluid flow and heat transfer interfacial conditions between a porous medium and a fluid layer. *Int. J. Heat and Mass Transfer* 2001; 44: 1735-1749.
- [11] Lee, D.Y., Vafai K. Analytical characterization and conceptual assessment of solid and fluid temperature differentials in porous media. *Int. J. Heat Mass Transfer* 1999; 42: 423–435.
- [12] Marafie, A., Vafai, K. Analysis of non-Darcian effects on temperature differentials in porous media. *Int. J. Heat Mass Transfer* 2001; 44: 4401-4411.